The Journal of Experimental Biology 206, 1059-1073

doi:10.1242/jeb.00209

The Kármán gait: novel body kinematics of rainbow trout swimming in a vortex street

James C. Liao[1,*], David N. Beal[2], George V. Lauder[3] and Michael S. Triantafyllou[4]

[1]*Department of Organismic and Evolutionary Biology, Harvard University, Cambridge, MA 02138, USA,*
[2]*Department of Ocean Engineering, Massachusetts Institute of Technology, Cambridge, MA 02139, USA,*
[3]*Department of Organismic and Evolutionary Biology, Harvard University, Cambridge, MA 02138, USA* and
[4]*Department of Ocean Engineering, Massachusetts Institute of Technology, Cambridge, MA 02139, USA*

*Author for correspondence (e-mail: jliao@oeb.harvard.edu)

Accepted 23 December 2002

Summary

Most fishes commonly experience unsteady flows and hydrodynamic perturbations during their lifetime. In this study, we provide evidence that rainbow trout *Oncorhynchus mykiss* voluntarily alter their body kinematics when interacting with vortices present in the environment that are not self-generated. To demonstrate this, we measured axial swimming kinematics in response to changes in known hydrodynamic wake characteristics. We compared trout swimming in the Kármán street behind different diameter cylinders (2.5 and 5 cm) at two flow speeds (2.5 and 4.5 $L\,s^{-1}$, where L is total body length) to trout swimming in the free stream and in the cylinder bow wake. Trout swimming behind cylinders adopt a distinctive, previously undescribed pattern of movement in order to hold station, which we term the Kármán gait. During this gait, body amplitudes and curvatures are much larger than those of trout swimming at an equivalent flow velocity in the absence of a cylinder. Tail-beat frequency is not only lower than might be expected for a trout swimming in the reduced flow behind a cylinder, but also matches the vortex shedding frequency of the cylinder. Therefore, in addition to choosing to be in the slower flow velocity offered behind a cylinder (drafting), trout are also altering their body kinematics to synchronize with the shed vortices (tuning), using a mechanism that may not involve propulsive locomotion. This behavior is most distinctive when cylinder diameter is large relative to fish length. While tuning, trout have a longer body wavelength than the prescribed wake wavelength, indicating that only certain regions of the body may need to be oriented in a consistent manner to the oncoming vortices. Our results suggest that fish can capture energy from vortices generated by the environment to maintain station in downstream flow. Interestingly, trout swimming in front of a cylinder display lower tail-beat amplitudes and body wave speeds than trout subjected to any of the other treatments, implying that the bow wake may be the most energetically favorable region for a fish to hold station near a cylinder.

Movies available on-line.

Key words: Kármán street, vortex street, drag wake, vortex, cylinder, hydrodynamic perturbation, swimming kinematics, rainbow trout, *Oncorhynchus mykiss*, Kármán gait, drafting, tuning, tacking, entraining.

Introduction

Historically, laboratory studies of fish locomotion have focused on steady swimming under micro-turbulent conditions to discern the fundamental principles of how fish move. This environmental simplification is necessary to understand the effects of three-dimensional movement for complex body and fin morphologies across swimming speeds and modes. Still, fish biologists acknowledge that steady swimming through low turbulence environments is not the dominant behavior of fishes, and in most cases represents only a small fraction of their daily behavioral routine (summarized in Webb, 1991). Turbulence is a ubiquitous phenomenon that fishes must contend with in nature, resulting from such varied sources as temperature differences, flow over inanimate structures, and vorticity generated by moving organisms.

Fishes swimming in flowing water often prefer to exploit turbulence associated with physical structures to reduce locomotory costs (Heggenes, 1988; Fausch, 1993; Webb, 1993; Gerstner, 1998; Gerstner and Webb, 1998; Webb, 1998a). Numerous field studies (Puckett and Dill, 1985; Heggenes, 1988, 2002; McMahon and Gordon, 1989; Shuler et al., 1994; McLaughlin and Noakes, 1998; Pavlov et al., 2000) attest to the strong ecological and commercial importance of understanding how fish interact with unsteady flow regimes. Fisheries scientists need to assess the impact of

hydrodynamic perturbations on migratory species in order to make management decisions about stream design, habitat management and fish passageways (Fausch, 1993; McLaughlin and Noakes, 1998). For engineers and biomechanists, recognizing how fish utilize heterogeneous flows could provide valuable insight into the governing principles of aquatic propulsion and stability.

Despite these applied and theoretical benefits, relatively few laboratory studies (but see Sutterlin and Waddy, 1975; Gerstner, 1998; Webb, 1998a) have quantitatively described the effects of hydrodynamic perturbations at the organismal level, in part because of the difficulty in generating and interpreting repeatable hydrodynamic perturbations. The wake behind simple geometric objects in a moving fluid, a subject well characterized by fluid mechanists, presents an attractive opportunity to generate consistent flow perturbations. By altering the dimensions of a given object, it is possible to manipulate vortical flows systematically to investigate their effect on swimming fish. In this study, we take advantage of the periodicity of vortex shedding behind a cylinder to generate repeatable hydrodynamic perturbations.

For Reynolds numbers between 300 and 150,000, flow past a stationary cylinder generates a staggered array of discrete, periodically shed, columnar vortices of alternating sign, collectively known as a vortex or Kármán street (Blevins, 1990). By changing flow velocity and cylinder diameter, it is possible to change the frequency of the Kármán vortices (vortex shedding frequency) and the wavelength that describes their spacing and size (wake wavelength).

Our goal is to use a controlled experimental system to contribute to an understanding of how swimming fish interact with hydrodynamic perturbations. We describe axial body kinematics of rainbow trout swimming behind different diameter cylinders at two different flow speeds and compare them to trout swimming in the free stream flow, and also describe the kinematics of trout swimming in the bow wake in front of a cylinder. Relative to the free stream, trout behind a cylinder invariably encounter lower flow velocity. We define the ability of a fish to use this region of reduced flow as ‘drafting’, and distinguish this from ‘entraining’, which describes the use of upstream flow in the suction region directly behind a cylinder to hold station (Webb, 1998a). We employ the term ‘tuning’ to describe the voluntary alteration of body kinematics to match a cyclical, external, hydrodynamic stimulus. Furthermore, we make the distinction that the mechanism for drafting and tuning may or may not be propulsive in nature. Although we could alter cylinder wake parameters, we could not separate the presence of the shed vortices from the phenomenon of reduced flow velocity in this study. Therefore, our goal is to determine if trout behind cylinders are tuning in addition to drafting. We test the hypothesis that trout are drafting with propulsive locomotion *versus* an alternative hypothesis in which trout are drafting using a non-propulsive mechanism of locomotion. If trout are only using the drag wake of the cylinder for its reduced flow, then tail-beat frequency and amplitude should be similar to trout swimming at free stream flows equivalent to the velocity deficit behind the cylinder. However, if trout are actually altering their body kinematics to reflect interaction with the vortices in the cylinder wake, then we expect that tail-beat frequency and body wavelength will match the corresponding vortex shedding frequency and wake wavelength of the cylinder, respectively, and that the general swimming kinematics will differ substantially from propulsive swimming kinematics in unobstructed flows.

Materials and methods

Animals

We obtained juvenile rainbow trout *Oncorhynchus mykiss* (Walbaum) from a commercial hatchery in western Massachusetts, USA. Fish were held in a 1200 liter circular freshwater tank (maintained at 15±1°C) with constant flow and fed commercial trout pellets daily. Eight trout, 10.0±0.3 cm total body length (L) and 10.0±0.5 g (mean ± S.E.M.), were used in the experiments.

Experimental procedures

Fish swam in an aerated, 600 liter recirculating flow tank (working section 28 cm×28 cm×80 cm) maintained at 15±1°C. We used 5.0 cm (large) and 2.5 cm (small) diameter, solid polyvinyl chloride cylinders cut in half lengthwise (D-section cylinders) to promote more discrete vortex shedding (Blevins, 1990). The projected areas of the large and small D-section cylinder (herein referred to simply as cylinder) were 18% and 9% of the cross-sectional area of the flow tank, respectively. Cylinders were secured in place from above with the lower end resting against the bottom of the flow tank to avoid self-oscillation (Fig. 1A). A RedLake high-speed digital video camera (250 frames s^{-1}, 1/500th s shutter speed) recorded the ventral view of the trout against a lighted background, which was accomplished by aiming the camera at a 45° front-surface mirror placed below the flow tank (Fig. 1). To minimize turbulence in the flow tank, water was directed through a baffle consisting of 6 mm diameter flow straighteners located approximately 50 cm upstream from the working section of the flow tank.

We specifically designed three ‘downstream’ cylinder treatments to identify the hydrodynamic variables that might be responsible for the kinematic behaviors observed (Fig. 2). Using the Strouhal number (0.2) appropriate for the Reynolds numbers of our experiment (5600–20,000 and 5000–40,000 using cylinder diameter and fish length, respectively; Blevins, 1990), we determined the expected vortex shedding frequency (f) according to the equation:

$$St = fd/U, \quad (1)$$

where St is Strouhal number, d is the cylinder diameter, and U is the flow velocity in the region of the cylinder. To account for flow constriction near the cylinder due to solid blocking effects, vortex shedding frequency was calculated above using the flow velocity:

$$U = U_f \times [W/(W - d)], \quad (2)$$

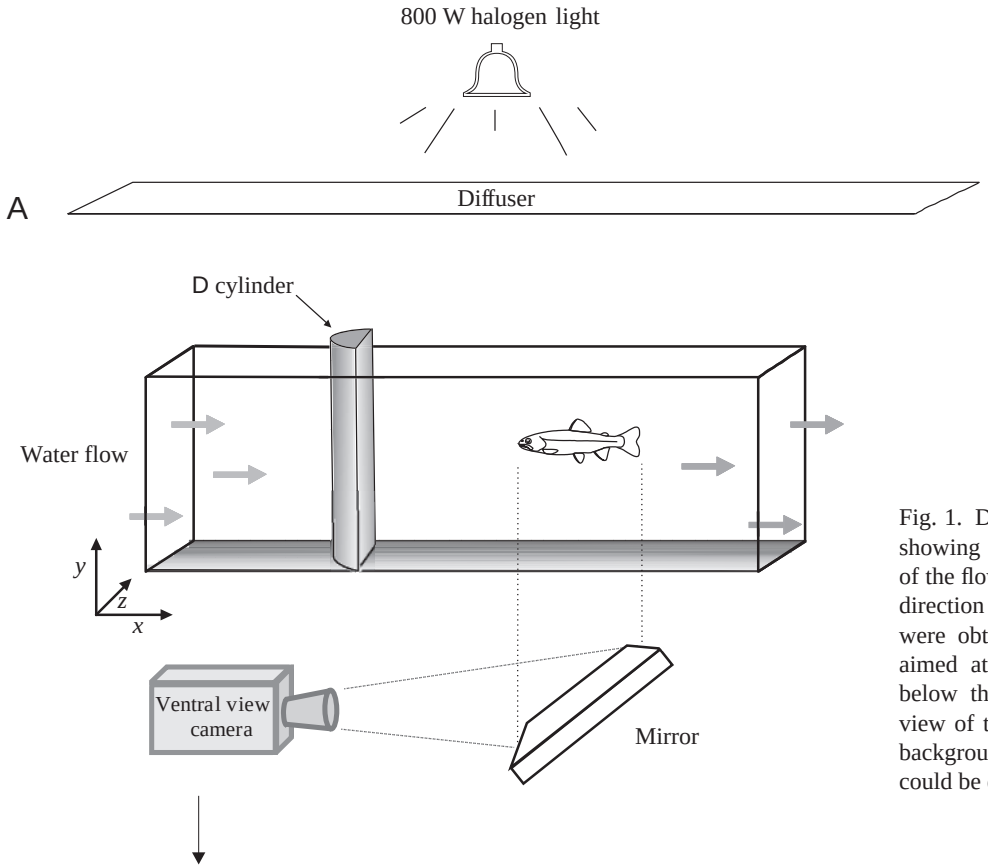

Fig. 1. Diagram of the experimental setup (A) showing a D-cylinder (not to scale) in the center of the flow tank with gray arrows representing the direction of water flow. Images of swimming fish were obtained with a high-speed video camera aimed at a 45° front-surface mirror positioned below the flow tank. An image of the ventral view of the fish (B) silhouetted against a lighted background provided a high-contrast image that could be digitized.

where U is the actual flow velocity in the region of the cylinder, U_f is the nominal flow velocity (2.5 or 4.5 $L\,s^{-1}$), and W is the width of the flow tank. We calculated the cylinder wake wavelength (λ), which describes the downstream spacing of the vortices, according to the equation:

$$\lambda = U_f/f. \quad (3)$$

Wake wavelength was calculated by dividing the nominal flow velocity by the constricted shedding frequency, because although the cylinder sheds vortices at a frequency determined by the constricted velocity, these vortices translate downstream at the nominal velocity.

Four of the five treatments were conducted at a free stream flow velocity of 4.5 $L\,s^{-1}$ (high flow): downstream of the small cylinder (smD4.5), downstream of the large cylinder (laD4.5), free stream (FS4.5), and bow wake in front of the large cylinder (BW4.5). The remaining treatment (smD2.5) consisted of a small cylinder at a velocity of 2.5 $L\,s^{-1}$ (low flow), and was designed to replicate the shedding frequency of the large cylinder at high flow, despite halving its wavelength and therefore decreasing the vortex spacing in the x direction (Fig. 2). For a given Strouhal number, vortex shedding frequency can be altered by cylinder diameter or flow speed (Equation 1). In contrast, by solving for f in Equation 1 and substituting into Equation 3, it is apparent that wake wavelength depends only on cylinder diameter. We were interested in testing the effect of vortex shedding frequency and wake wavelength on fish swimming, so we designed flow velocity and cylinder diameter combinations for our treatments to hold one wake parameter constant while varying the other. For example, subjecting trout to two different speeds using the same cylinder allowed us to observe differences in swimming kinematics caused by changing the vortex shedding frequency without changing the wake wavelength (Fig. 2A,B).

The high and low flow velocities were chosen because they allowed manipulation of cylinder wake variables, elicited recognizable, stereotypical body kinematics, and were within the range of swimming speeds attained by trout swimming behind boulders and woody debris in the field (Heggenes, 1988; McMahon and Gordon, 1989; Shuler et al., 1994). For

all treatments, we analyzed only those sequences in which fish were swimming more than 0.3 *L* above the bottom of the flow tank. Because cylinders were positioned in the middle of the flow tank, all swimming sequences by necessity were obtained with the fish at least 1 *L* away from the side walls.

We used digital particle image velocimetry (DPIV) to verify the presence of a Kármán street behind the cylinders, confirm calculated shedding frequencies and wake wavelengths, and make measurements of the reduced flow (velocity deficit) in the center of the wake. Silver-coated glass spheres (12 μm diameter) were seeded in the flow tank and illuminated by a horizontal light sheet (15 cm×28 cm×0.1 cm) generated by an 8 W argon-ion Coherent laser. Two-frame cross-correlation analysis of particle images recorded 4 ms apart yielded a 31×36 matrix of 1116 velocity vectors, from which a plot of vorticity was generated and overlaid (Fig. 3A; Insight version 3.0 software, TSI Inc., St. Paul, MN, USA). DPIV procedures follow those used previously to study locomotor hydrodynamics in freely swimming fishes (Drucker and Lauder, 1999; Liao and Lauder, 2000; Wilga and Lauder, 2000; Nauen and Lauder, 2002). At approximately the same distance (20 cm) and height (5 cm) that fish were observed holding station downstream from the large cylinder, a single row of 36 velocity vectors (Fig. 3A, white arrows) along the *z* direction was averaged for 103 continuous video frames (in the absence of a fish), representing a random, 8 s sequence of the wake (Fig. 3B). Predicted values of vortex shedding frequency and wavelength (Equations 1–3) were verified by statistical comparison to empirically derived values based on visual selection of vortex centers.

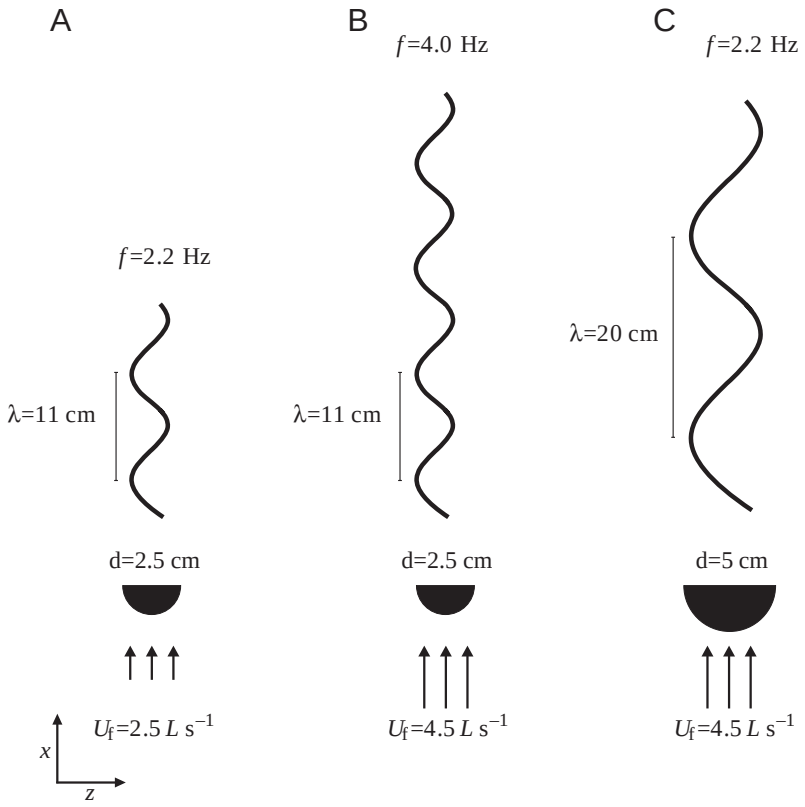

Fig. 2. Diagram of the experimental design showing the effect of cylinder diameter and flow speed on vortex shedding frequency and wake wavelength. Objects are not drawn to scale. (A) The small, 2.5 cm diameter (d) D-cylinder in low flow (ambient flow speed is set at 2.5 $L\,s^{-1}$ prior to solid blocking effects) has a low shedding frequency *f* (2.2 Hz) and a short wavelength λ (11 cm). (B) Using the same cylinder and increasing the ambient flow velocity to 4.5 $L\,s^{-1}$, the shedding frequency almost doubles (4.0 Hz) but the wavelength remains the same. (C) Using the large, 5 cm diameter D-cylinder at high flow results in a shedding frequency of 2.2 Hz, which is the same as in A, except that for the large cylinder the wake wavelength almost doubles (20 cm), representing a substantial difference in downstream–upstream vortex spacing. Vortex shedding frequency can be changed by altering cylinder size or flow speed, while wavelength depends only on cylinder diameter. Shedding frequency and wavelength values reported are calculated from constricted flow velocities (*U*; see Materials and methods). U_f, nominal flow velocity – see text.

From the video sequences, we measured tail-beat frequency, wavelength, wave velocity, magnitude and location of maximum body curvature, maximum amplitude of four body locations (snout, center of mass, 50% *L* and tail), maximum head angle and downstream distance from snout to cylinder. Tail-beat frequency was determined by averaging the number of tail-beat oscillations over a known time (at least four oscillations per individual). Body wavelength was calculated according to Equation 3 by substituting the length-specific body wave speed (*V*, obtained by measuring the average speed of the maxima moving down the midline) for the nominal flow velocity (U_f) and the tail-beat frequency for the vortex shedding frequency (*f*). The four body locations were selected to provide a general indication of the effects of different cylinder wakes on longitudinal body kinematics. Amplitudes at these four points were measured as the maximum lateral excursion from the midline. We experimentally determined the center of mass (COM) *post-mortem* for straight-stretched fish by iteratively balancing the body between right and left side pins. Head angle was calculated as the maximum angle of the head relative to the axis of the free stream flow. In addition, we calculated slip as U_f/V, where U_f is taken to be the length-specific swimming velocity of the fish. Strouhal numbers for swimming trout were calculated according to Equation 2 by substituting tail-beat frequency for vortex shedding frequency (*f*) and tail-beat amplitude (using peak-to-peak amplitude; as in Triantafyllou et al., 2000) for cylinder diameter (d).

Image analysis

For all treatments, at least 20 video frames (separated in time by 12–20 ms, depending on the swimming speed of the fish) were captured for each fish for each of four tail-beat trials. We used

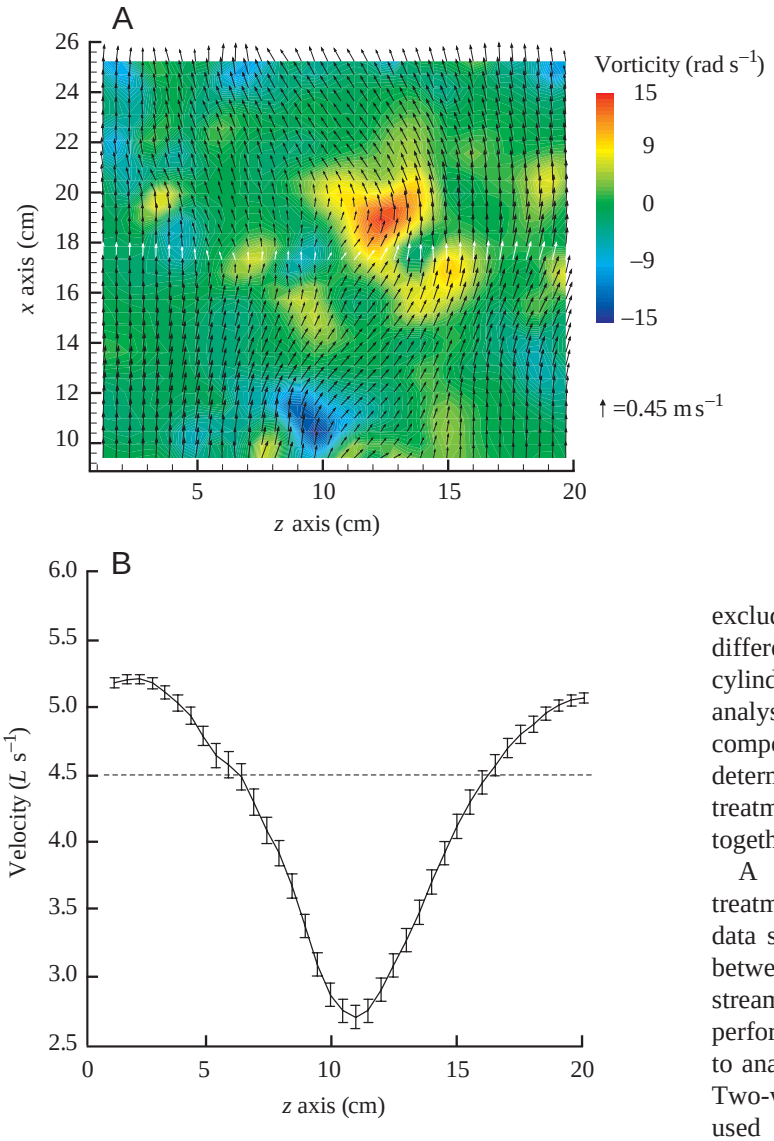

Fig. 3. (A) Superimposed vorticity and velocity vector plot of the wake in the region that trout were observed holding station downstream behind the 5 cm cylinder at 4.5 L s^{-1}. The color plot represents vorticity and the length and orientation of the arrows represents velocity magnitude and direction. The single row of white arrows represents the region of the wake in which vectors were selected for statistical analysis of the velocity in (B). Flow is from bottom to top. One counterclockwise vortex (red) has been shed into the middle of the frame and a second, clockwise vortex (blue) has just entered the field of view. Two centers of vorticity are shed per period to form the Kármán street, with a wavelength of 20.30±0.43 cm (mean ± S.E.M., N=29). (B) Time-averaged velocity profile of the downstream flow component (x direction) reveals that the minimum velocity in the wake (2.7±0.2 L s^{-1}; mean ± S.E.M., N=103) is over half the free stream velocity (4.5 L s^{-1}).

an automated digitizing program written in Matlab v6.1 to digitize 20 points on each side of the axial body silhouette, thresholding out interferences with fin profiles, for a total of 40 points per image. After a series of cubic spline functions were fitted to these outline points, a midline spline was constructed and then divided into 20 segments, the longitudinal positions of each which were recorded as relative body lengths (as in Jayne and Lauder, 1995).

Statistical tests

Means and standard errors were calculated for all kinematic variables associated with swimming. Two-sample unpaired t-tests were conducted to see if tail-beat frequency differed from vortex shedding frequency and if body wavelength differed from wake wavelength. All statistical tests were performed at an α level of 0.05.

A principal-components analysis determined which of the kinematic variables contributed to most of the variation in the entire data set. Data from the bow wake treatment were excluded since we were primarily interested in detecting differences in swimming kinematics between downstream cylinder treatments and free stream swimming. A multivariate analysis of variance (MANOVA) was performed on principal component 1 (PC1) and principal component 2 (PC2) to determine if there were significant differences among treatment means when all kinematic variables were considered together.

A MANOVA and subsequent *post-hoc* tests on all treatments except the bow wake (to make maximum use of the data set, 7 individuals) determined if there were differences between the downstream cylinder treatments and the free stream treatment as well as within cylinder treatments. We performed a MANOVA on all five treatments (4 individuals) to analyze bow wake data in the context of other treatments. Two-way, mixed-model analyses of variance (ANOVA) were used to determine the effects of individual (random) and cylinder treatment (fixed) on the kinematic variables. The F value of the fixed effect was calculated as the mean square of the fixed effect over the interaction term of the random effect and the fixed effect. To account for multiple simultaneous ANOVAs, the level of significance was adjusted within columns using the sequential Bonferroni technique (Rice, 1989). Where appropriate, we note when P values are less than 0.05 but do not meet the Bonferroni adjusted significance value. For all kinematic variables, we recorded 3–4 tail-beat cycles for each fish for each treatment. Statistical tests were performed by Systat (version 4.5 for the PC), Statview (version 5.0.1 for the PC), or calculated from Zar (1999).

Results

General observations of drafting behind a cylinder

At a flow velocity of 2 L s^{-1} or lower, trout typically swim more than 3 L downstream of a cylinder and close to one of the side walls of the flow tank. Within minutes of increasing the flow to 4.5 L s^{-1}, trout advance upstream and center themselves

approximately 2 *L* behind the cylinder and between 0.1 and 1 *L* above the bottom of the flow tank. Trout hold station at a consistent distance behind a cylinder for the remainder of an experimental treatment (1–3 h) using a visually distinctive pattern of locomotion. This behavior is usually not continuous for more than six consecutive tail oscillations, being interrupted by corrective tail motions of small amplitude and high frequency. Even without these corrective motions, fish do not always oscillate their tails symmetrically while holding station. Fish occasionally leave the wake to investigate particles mistaken for food, only to return immediately to the same position behind the cylinder. At the beginning of an experiment, trout advancing too close to the cylinder (<1 *L*) are drawn rapidly upstream, often hitting the cylinder. The occurrence of this behavior was most noticeable for fish behind the large cylinder, and decreased as an experiment progressed. Although the ambient flow velocity was set at 4.5 $L\,s^{-1}$ for the large cylinder treatment, due to the direction of fluid rotation at the outside edge of the wake, the flow velocity increases 16% to a maximum of 5.2±0.1 $L\,s^{-1}$ (mean ± S.E.M.). Conversely, in the center of the wake vortical flow is directed upstream relative to the free stream velocity, though overall

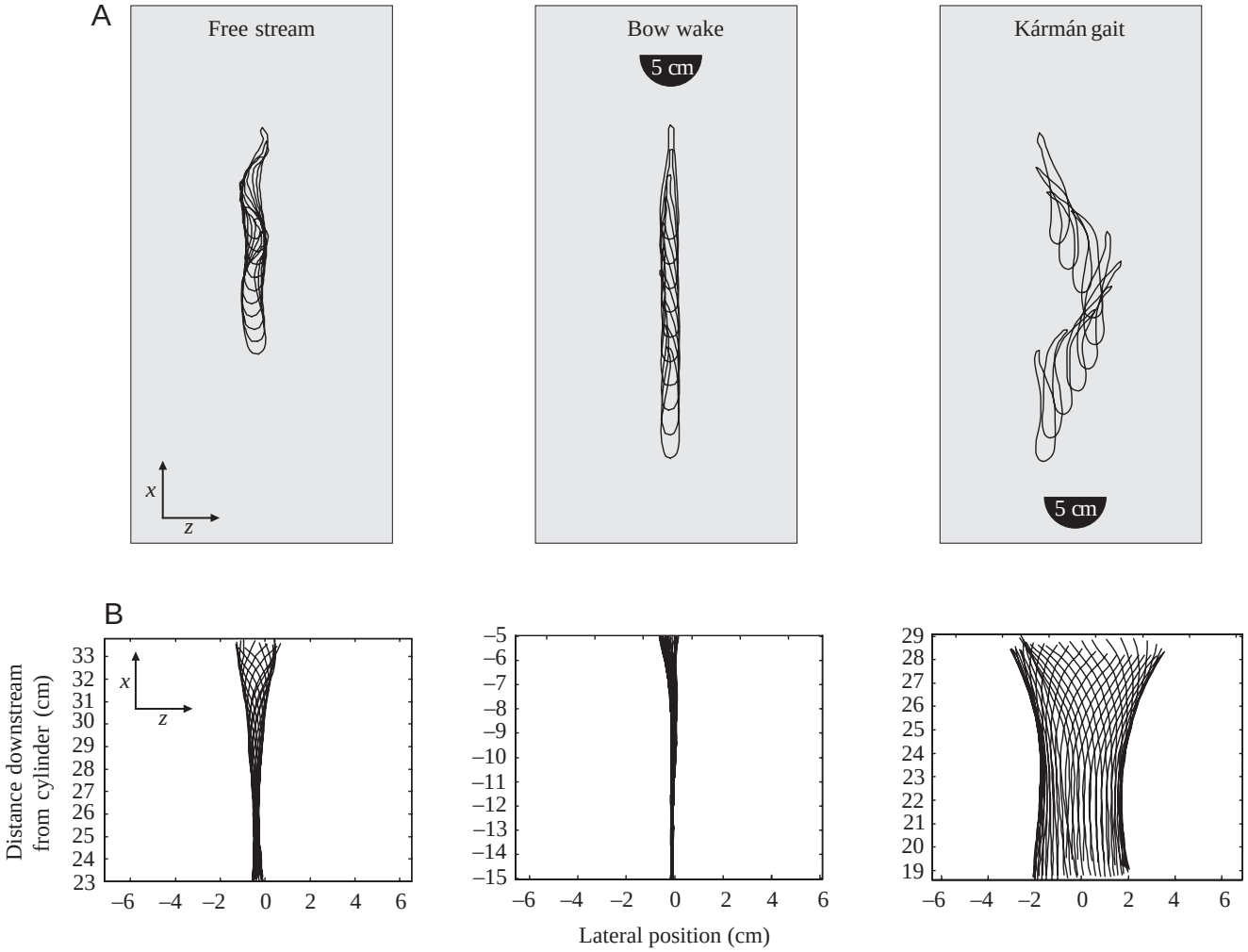

Fig. 4. Superimposed body outlines (A) and body midlines (B) for three treatment conditions, from left to right; free stream or 'no cylinder' treatment, bow wake treatment in front of a 5 cm D-cylinder, and downstream treatment behind the 5 cm D-cylinder, illustrating the Kármán gait. The ten body outlines for each treatment (A) showing approximately one tail-beat cycle were recorded at intervals of 24 ms, 48 ms and 48 ms, respectively. Spacing along the *x* direction between successive outlines reflects relative swimming velocities. Superimposed midlines (B) show the motion of the body at higher time resolution for the three treatments. The distance of the fish relative to the downstream edge of the cylinder (where the downstream edge of the cylinder is zero, the region upstream of the cylinder is negative, and downstream of the cylinder is positive) is given on the *x*-axis, while the lateral position of the fish relative to the center of the cylinder is given on the *z*-axis. For the free stream treatment, values on the *x*-axis illustrate the position of the trout relative to a fixed point upstream (approximately 2.5 *L* downstream of where the cylinder would be located for other treatments). Therefore, during the free stream treatment fish hold station about a half body length further downstream in the flow tank than during cylinder treatments. The tip of the caudal fin for a fish swimming in the bow wake is positioned 5 cm upstream from the downstream edge of the cylinder, or 2.5 cm in front of the cylinder.

there is still a net downstream fluid movement that manifests itself in the form of a sinusoidal region of reduced flow ($2.7\pm0.2\,L\,s^{-1}$, Fig. 3B).

Holding station behind cylinders versus *free stream swimming*

Trout holding station behind a cylinder display unique axial body kinematics that are readily distinguishable from steadily swimming trout using active undulatory propulsion in the absence of a cylinder (Fig. 4). In general, trout holding station behind a cylinder appear passive, resembling the motion of a flag flapping slowly in the wind. Compared to trout swimming in the free stream at $4.5\,L\,s^{-1}$, trout holding station behind the large cylinder at the same speed show a 303% decrease in tail-beat frequency and a 354% increase in body wavelength (Fig. 5). In addition, body amplitudes increase 300–800% (depending on the body point), owing to the lateral translation of the entire body in the wake (Figs 4, 6). All body amplitudes increase significantly ($P<0.001$) for trout behind the large cylinder as compared to trout swimming in the free stream. For

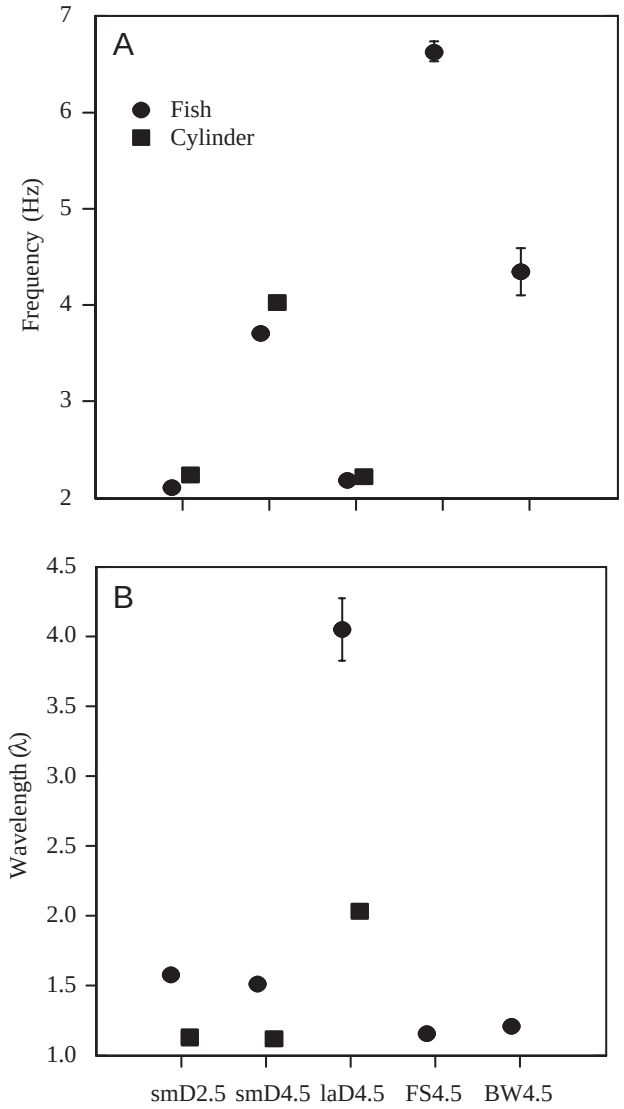

Fig. 5. Mean tail-beat frequency (A) and normalized body wavelength (B) for each of the five treatments (smD2.5 is the small D-cylinder at $2.5\,L\,s^{-1}$, smD4.5 is the small D-cylinder at $4.5\,L\,s^{-1}$, laD4.5 is the large D-cylinder at $4.5\,L\,s^{-1}$, FS4.5 is the free stream at $4.5\,L\,s^{-1}$, and BW4.5 is the bow wake in front of the large cylinder at $4.5\,L\,s^{-1}$, where L is the total length of the fish). Values are means ± S.E.M., but in most instances the error bars are small enough to be obscured by the data symbol. Circles represent fish data (A) and squares represent cylinder data (see text for calculation). For all three downstream cylinder treatments, the tail-beat frequency is similar to the vortex shedding frequency and the fish adopts a body wavelength that is longer than the cylinder wake wavelength.

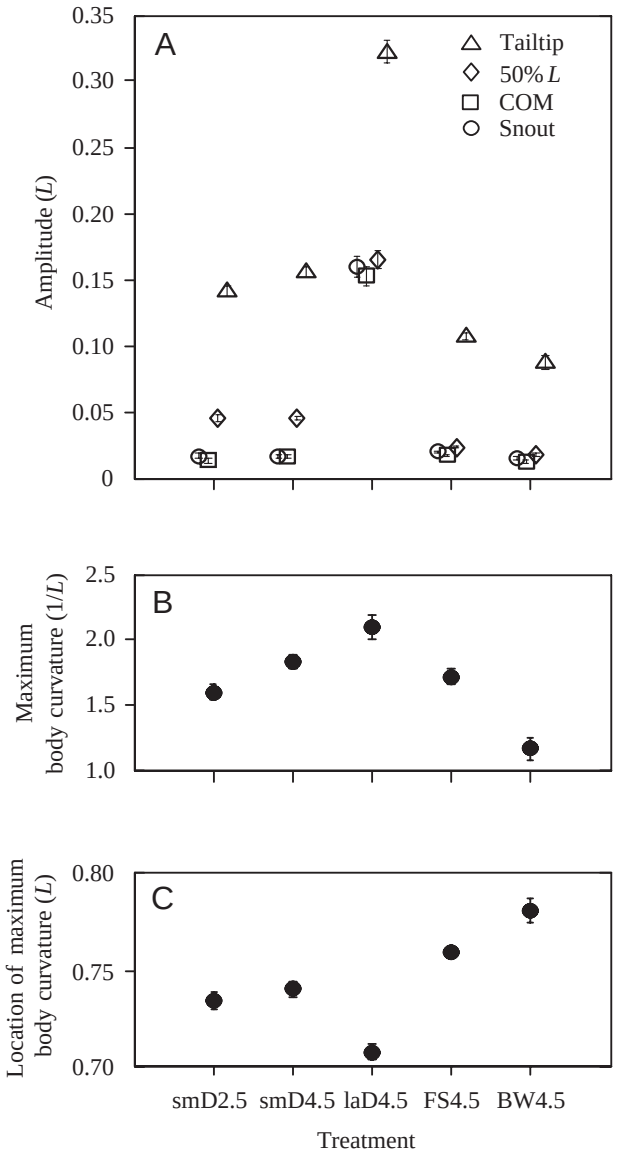

Fig. 6. (A) Lateral body amplitudes taken relative to the midline at four locations. Circles represent the snout; squares, the center of mass (COM); diamonds, a point 50% down the body; triangles, the tail tip. (B) Maximum curvatures and (C) their corresponding positions along the body. Trout behind the large cylinder have the largest and most anteriorly located body curvatures, while trout in the bow wake have the smallest and most posteriorly located curvatures.

Table 1. *Summary statistics of cylinder wake variables and trout kinematic variables for five experimental treatments*

Variable	smD2.5	smD4.5	laD4.5	FS	BW
Vortex shedding frequency (Hz)	2.24±0.01	4.02±0.02	2.22±0.01	–	–
Tail-beat frequency (Hz)	2.10±0.04	3.71±0.05	2.18±0.05*	6.62±0.11	4.34±0.24
Cylinder wake wavelength (*L*)	1.12±0.01	1.12±0.01	2.03±0.01	–	–
Body wavelength (*L*)	1.57±0.04	1.50±0.03	4.05±0.22	1.15±0.02	1.21±0.03
Snout amplitude (*L*)	0.02±0.01	0.02±0.01	0.16±0.02	0.02±0.01	0.02±0.01
COM amplitude (*L*)	0.01±0.01	0.02±0.01	0.15±0.01	0.02±0.01	0.01±0.01
50% *L* amplitude (*L*)	0.05±0.01	0.05±0.01	0.17±0.01	0.02±0.01	0.02±0.01
Tail-beat amplitude (*L*)	0.14±0.01	0.16±0.01	0.32±0.02	0.11±0.01	0.09±0.01
Max. body curvature (1/*L*)	1.60±0.06	1.83±0.06	2.09±0.09	1.71±0.06	1.16±0.09
Location of max. curvature (*L*)	0.74±0.01	0.74±0.01	0.71±0.01	0.76±0.01	0.78±0.01
Distance downstream from cylinder (*L*)	1.68±0.03	1.77±0.05	1.92±0.05	–	–
Maximum head angle (degrees)	16.53±0.54	14.74±0.49	16.76±0.96	12.96±0.40	10.46±0.65
Slip	0.77±0.02	0.82±0.01	0.55±0.02	0.60±0.01	0.93±0.06
Strouhal number	0.24±0.01	0.26±0.01	0.31±0.01	0.32±0.01	0.17±0.01

Values are means ± S.E.M. (N=8 for all treatments except for BW, N=5).

L, total body length.

*Not significantly different from the corresponding vortex shedding frequency (P=0.48).

Treatments: smD2.5, 2.5 cm diameter cylinder at 2.5 $L\,s^{-1}$; smD4.5, 2.5 cm diameter cylinder at 4.5 $L\,s^{-1}$; laD4.5, 5 cm diameter cylinder at 4.5 $L\,s^{-1}$; FS, free stream at 4.5 $L\,s^{-1}$; BW, bar wake of 5 cm diameter cylinder at 4.5 $L\,s^{-1}$.

trout behind small cylinders, the increase in the snout and COM amplitude is greater relative to the posterior half of the body compared to trout swimming in the free stream (Table 1). Irrespective of flow velocity, trout behind a small cylinder display larger midbody and tail amplitudes (P<0.002, Table 1) than those of trout in the free stream, but have similar snout and COM amplitudes (P=0.68, P=0.59, respectively). Maximum body curvature for trout behind the large cylinder is not statistically different from that of trout swimming in the free stream (P=0.054, Fig. 6), though the absolute radius of curvature is larger. Compared to trout swimming with active undulatory propulsion in the free stream, the location of maximum curvature is closer to the head for trout holding station behind cylinders (P<0.05, N=108). Trout behind the large cylinder at high flow and the small cylinder at low flow have larger head angles than free stream swimming trout (P<0.001, Fig. 7).

Traditional metrics of fish swimming efficiency further illustrate how swimming behind a cylinder differs from swimming in the free stream. Trout behind the large cylinder have a lower slip value, resulting from a higher body wave speed, than trout swimming in the free stream at 4.5 $L\,s^{-1}$ (P=0.001, N=108, Fig. 8A). By contrast, the body wave speeds for trout behind the small cylinders are lower than that for trout swimming in the free stream, resulting in higher slip values (P=0.001, N=108, Fig. 8A). The Strouhal number for trout holding station behind a large cylinder is not statistically different from that of a trout swimming in the free stream. In comparison, trout holding station behind small cylinders have much lower Strouhal numbers (Fig. 8B).

Locomotor kinematics behind different cylinder treatments

Trout alter their axial swimming kinematics to reflect the hydrodynamic characteristics of the cylinder wake. We found that trout generally match their tail-beat frequency to the expected vortex shedding frequency for all three downstream cylinder treatments (see Fig. 5 and Table 1). Trout behind cylinders have a body wavelength that is always longer than the corresponding wake wavelength (P<0.05, N=108; Table 1). For example, behind the large cylinder the body wavelength (41 cm) is more than twice as long as the wake wavelength (20 cm; Figs 2, 5). Body wavelength differs among trout behind the large and small cylinders (P<0.001, N=108) but not between the two small cylinder treatments (P=0.19, N=108, Fig. 2), reflecting the relationships in wake wavelength. There is a larger difference between the body and wake wavelengths for trout behind the large cylinder treatment than for trout behind the small cylinder treatments. Comparisons among the three downstream cylinder treatments reveal that trout do not match their body wave speed to the speed at which they encounter shed vortices.

Regardless of flow speed, trout behind the small cylinder have body amplitudes that are not statistically different from each other (P≥0.37, N=108, Fig. 6A), indicating that shedding frequency does not affect body amplitude. These body amplitudes behind the small cylinders are, in turn, much smaller than that of trout behind the large cylinder (P<0.001, N=108). The amplitude of the snout, COM and midbody are similar for trout behind the large cylinder, while the tail-beat amplitude is about twice this magnitude. Trout subjected to the small cylinder treatments have snout amplitudes that are similar to the COM amplitude, but much larger midbody and the tail-tip amplitudes (3× and 10×, respectively), resulting in a steeper amplitude envelope than seen in trout swimming behind the large cylinder.

The degree and location of body bending depends on the size

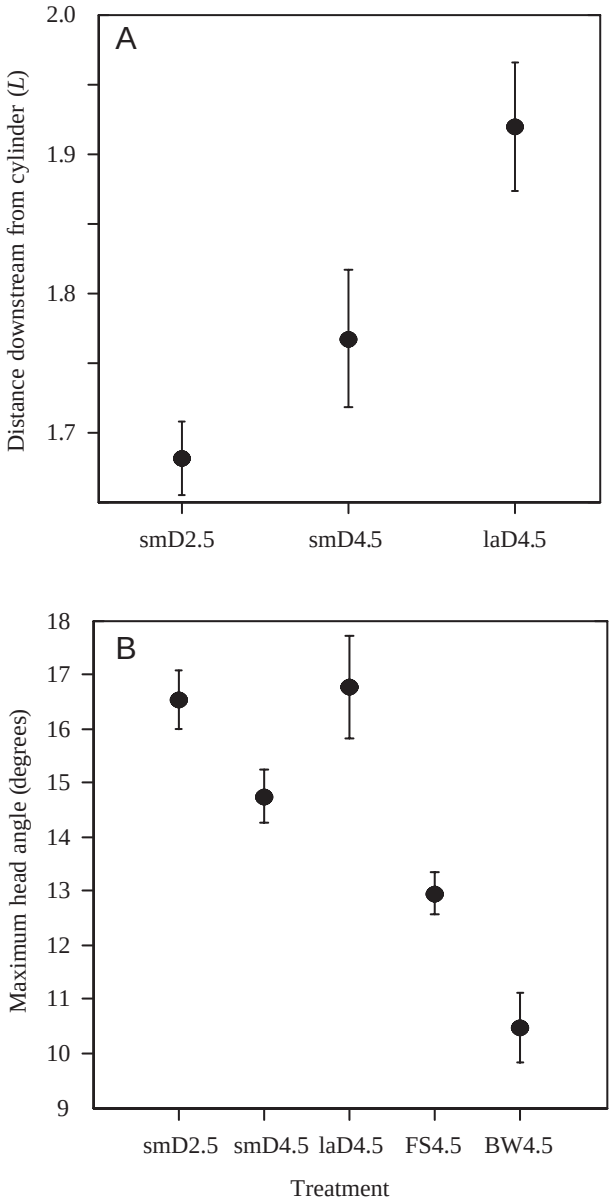

Fig. 7. (A) Distance from the tip of the snout to the downstream edge of the D-cylinder for the three downstream cylinder treatments. Fish are located furthest downstream from the laD4.5 treatment, followed by the smD4.5 and smD2.5 treatments. (B) Mean maximum head angle relative to the axis of free stream flow. Head angles are higher for trout behind cylinders than for trout swimming in the free stream and the bow wake. Head angles are not statistically different between the cylinder treatments that have the same vortex shedding frequency but different wavelengths (smD2.5 and laD4.5), and are different between the treatments that have different shedding frequencies but the same wavelength (smD2.5 and smD4.5).

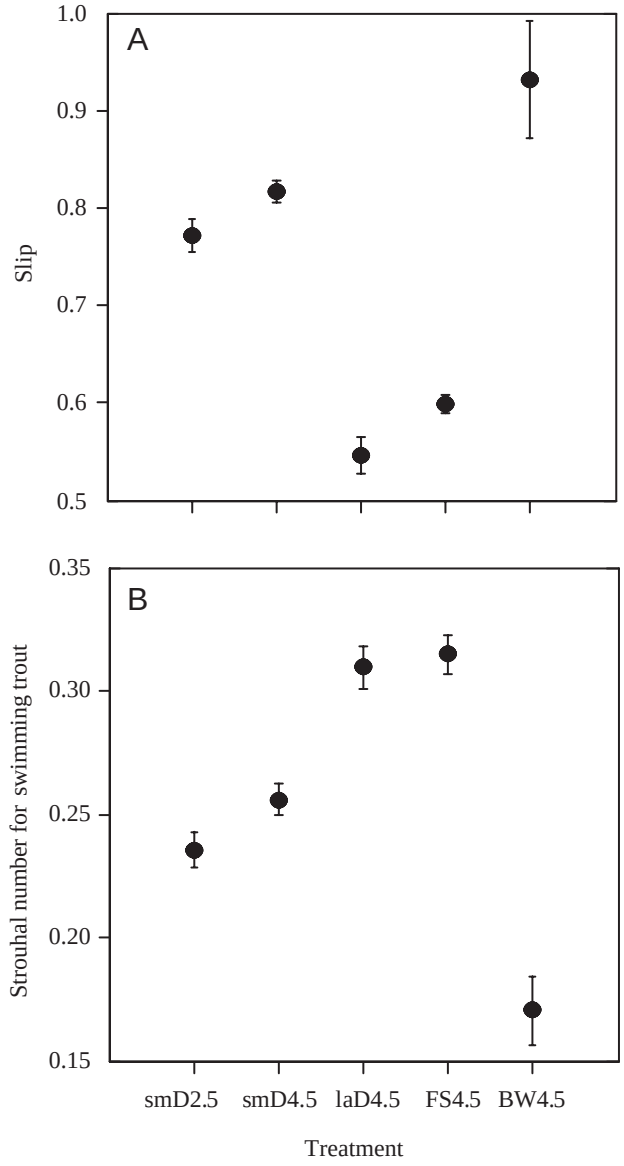

Fig. 8. Slip (A) and Strouhal number (B) for all five experimental treatments. (A) A low slip value, such as that for fish displaying the Kármán gait behind the large cylinder, indicate that the body wave velocity is relatively greater than the swimming velocity of the fish. For the slip values shown here, swimming velocities were taken as the free stream velocity and not the reduced velocity behind the cylinder. A high slip value for trout swimming in the bow wake suggests a high mechanical swimming efficiency. (B) Strouhal number for trout swimming behind the large cylinder is not statistically different from the Strouhal number for free stream swimming fish. Strouhal number is significantly lower for fish swimming in the bow wake. See Discussion for the appropriateness of measuring slip and Strouhal number for fish swimming behind and in front of cylinders.

and strength of the shed vortices and not on the frequency of vortex shedding. Maximum curvature along the body of the trout does not track cylinder diameter or flow speed individually; only a combination of the two causes larger body curvatures. For example, the maximum body curvature for trout behind the large cylinder is not significantly different from that of trout behind the small cylinder at high flow (Fig. 6B), but is higher than for trout behind the small cylinder at low flow ($P<0.05$, $N=108$, Fig. 6B,C; Table 2). Likewise, the maximum body curvatures for trout behind the small cylinder treatments at two different flow speeds are not

Table 2. *Results from a two-way ANOVA of the effects of individual and treatment on swimming kinematic variables*

Variable	Individual (6,80)	Treatment (3,18)	Individual × treatment (18,80)	Summary of pairwise Bonferroni–Dunn *post-hoc* probability matrix
Tail-beat frequency (Hz)	6.7**	317.9**	4.7**	FS>smD4.5>smD2.5=laD4.5
Body wavelength (*L*)	0.8	77.5**	1.3	laD4.5>smD2.5=smD4.5>FS
Snout amplitude (*L*)	1.6	198.4**	1.4	laD4.5>smD2.5=smD4.5=FS
COM amplitude (*L*)	1.3	178.0**	1.8	laD4.5>smD2.5=smD4.5=FS
50% *L* amplitude (*L*)	2.2	192.7**	1.9	laD4.5>smD2.5=smD4.5>FS
Tail-beat amplitude (*L*)	3.6*	261.9**	1.3	laD4.5>smD4.5>smD2.5>FS
Max. body curvature (1/*L*)	2.4	5.8*	0.8	laD4.5>smD2.5, smD2.5=smD4.5=FS, smD4.5=laD4.5
Location of max. curvature (*L*)	5.2**	5.3*	1.0	FS>smD2.5=smD4.5>laD4.5
Distance downstream from cylinder (*L*)	7.9** (6,60)†	1.3 (2,12)†	5.6** (12,60)†	–
Maximum head angle (degrees)	5.1**	5.2*	1.8	smD2.5=smD4.5=laD4.5>FS, smD4.5=FS

Data are from 7 individuals (3–4 cycles per individual for each treatment). To increase statistical power in the analyses of downstream cylinder treatments, bow wake data were excluded.

Table entries are *F*-values, with degrees of freedom in parentheses in the column heading.

*Significant at $P \leq 0.05$ or **$P \leq 0.005$, using the sequential Bonferroni method (Rice, 1989).

†Degrees of freedom for downstream cylinder distances.

Treatments: smD2.5, 2.5 cm diameter cylinder at $2.5\,L\,s^{-1}$; smD4.5, 2.5 cm diameter cylinder at $4.5\,L\,s^{-1}$; laD4.5, 5 cm diameter cylinder at $4.5\,L\,s^{-1}$; FS, free stream at $4.5\,L\,s^{-1}$.

statistically different ($P<0.05$, $N=108$, Fig. 6B,C; Table 2). Thus, when flow speed is held constant, trout behind the large cylinder do not bend their body to a greater degree than trout behind the small cylinder; the only difference is that trout behind the large cylinder use more of the body to participate in the curvature. Of the three downstream cylinder treatments, maximum body curvature is closest to the tail for trout behind the small cylinder, high flow treatment, and closest to the head for trout behind the large cylinder ($P<0.05$, $N=108$, Fig. 6C). Longitudinal position of maximum body curvature does not vary with flow speed, as shown by comparing the values from the two small cylinder treatments. Thus, the degree of maximum body curvature depends on the size and strength of the vortices generated by the combination of cylinder diameter and flow speed, while the location of maximum curvature depends only on the cylinder diameter.

Additional locomotor variables illustrate that trout behind cylinders are reacting to wake parameters. Trout hold station further downstream from the large cylinder treatment than the small cylinder treatment at low flow ($P<0.005$, $N=81$); however, downstream distances are not different between other treatments ($P \geq 0.1157$, $N=81$, Fig. 7A). The two treatments that generate the lowest vortex shedding frequency (smD2.5 and laD4.5, Fig. 7B) also elicit the largest head angles (which are not statistically different from each other). Body wave speed increases with the combination of increased cylinder diameter and flow velocity, and is not affected by either variable individually ($P=0.001$, $N=108$). Specifically, trout behind the large cylinder have a faster body wave than trout behind the small cylinder at high flow, which in turn have a faster body wave than the small cylinder at low flow ($P=0.001$, $N=108$). This generates a low slip value for trout behind the large cylinder (Fig. 8). Strouhal numbers for all high flow treatments, with the exception of the bow wake, fall within the range 0.25–0.35.

Locomotor kinematics in the bow wake versus *free stream*

Only certain kinematic parameters differ between trout swimming in front of a cylinder and trout swimming in the free stream after Bonferroni adjustment. Trout in the bow wake have a much lower tail-beat frequency than trout swimming in the free stream ($P<0.0001$, $N=79$, Fig. 5A). Although trout in the bow wake (Figs 4, 6) have body amplitudes that are not different than trout swimming in the free stream after Bonferroni adjustment, they have lower tail-beat amplitudes ($P<0.05$, $N=79$) prior to Bonferroni adjustment. Likewise, maximum body curvature is significantly lower ($P<0.05$, $N=79$) for fish in the bow wake only prior to Bonferroni adjustment. Maximum body curvature is located further posteriorly along the body for bow wake fish than for free stream fish ($P<0.005$, $N=79$, Fig. 6). Fish swimming in the bow wake do not have a smaller maximum head angle after Bonferroni adjustment. Although body wavelength is not statistically different between the two treatments, the speed at which this wave passes down the body is much lower ($P<0.0001$, $N=79$) and more variable for fish swimming in the bow wake, thus generating a higher slip value (Fig. 7). Strouhal number for the bow wake is 0.17, the lowest of all treatments.

Principal components analysis

A principal components analysis on 13 kinematic variables

for all treatments except the bow wake indicated that PC1 and PC2 accounted for 50% and 18% of the total variation and in the dataset, respectively (Fig. 9). The variables most responsible for separating out the treatments along PC1 were body wavelength and body amplitude, while the variables most responsible for separating out the treatments along PC2 were tail-beat frequency, body wave speed, and location of minimum amplitude. Performing a MANOVA on these scores indicated a highly significant difference among the treatment means (Wilks' lambda F=23.94, P=0.004). *Post-hoc* tests indicate that for PC1 all treatment means were different (P<0.05, N=108) except between the two small cylinder treatments (Fig. 9). For PC2, all treatment means were different (P<0.005, N=108) except between the small cylinder and large cylinder at high flow speed.

Discussion

A novel gait behind cylinders

Trout swimming behind cylinders adopt a unique pattern of axial body motion that we term the Kármán gait after Theodore von Kármán, the fluid dynamicist who, in 1912, formally described the stable street of staggered vortices behind cylinders (see Blevins, 1990). It is generally accepted that locomotor styles that differ fundamentally in mechanics are distinguished as different gaits. Our criteria for naming this behavior a gait are based on previous definitions and ideas on animal movement through fluids (Blake, 1983; Alexander, 1989; Rayner, 1995; Webb, 1998b; Tobalske, 2000). We believe that the kinematic differences between the Kármán gait and free stream swimming are at least as dramatic as those separating classical terrestrial gaits (Alexander, 1989). We propose that trout adopting the Kármán gait reduce locomotor costs by altering their body kinematics to capture energy from the low-pressure, high-vorticity regions in the cylinder wake.

Previous studies using smaller cylinders (Sutterlin and Waddy, 1975; Webb, 1998a) found that fish entrain (hold station using upstream flow) with their head just behind and to one side of a cylinder. In addition to several biotic factors (Webb, 1998a), entraining may depend on the ratio of cylinder diameter to fish length, which at 1:12 (Sutterlin and Waddy, 1975) is much smaller than for the large cylinder treatment in this study (1:2). The proximity of the body to the cylinder in these earlier studies (Sutterlin and Waddy, 1975; Webb, 1998a) indicates that fish were taking advantage of actual upstream flow in the low-pressure region directly behind the cylinder (Vogel, 1994; Zdravkovich, 1997). In addition, the proximity of the fish to the cylinder can disrupt the vortex shedding frequency and may be responsible for the aperiodic body movements observed. Station holding strategies may also differ with species. Trout in this study position themselves further downstream from a cylinder compared to river chub and smallmouth bass, despite a similar cylinder diameter to fish length ratio (1:4) and swimming speed (3.5–4.5 $L\,s^{-1}$; Webb, 1998a).

Given our experimental conditions, trout do not entrain in the suction region behind cylinders. Instead, they hold station far enough away from the cylinder that the net flow they experience is always directed downstream. Trout choose not to position themselves close to the cylinder (<1 L) because the average low-pressure region, which extends less than two diameters downstream from the cylinder (Gerrard, 1966), is strong enough to draw them into contact with the cylinder and thereby disrupt their station holding behavior. The distance where trout hold station behind the large cylinder coincides with the region in which the Kármán vortices are fully formed; depending on the Reynolds number, this is 3–5 cylinder diameters or 1.5–2.5 L downstream of the cylinder (Weihs, 1973; Zdravkovich, 1997; Fish, 1999). Our data show a tendency for trout to hold station further downstream as cylinder diameter and flow speed increase (Fig. 7A).

We propose that the onset of the Kármán gait coincides with the hydrodynamic stability and strength of the cylinder wake. By using long, fine-diameter flow straighteners and large D-cylinders, we able to generate a relatively stable vortex street (verified by DPIV) at these high Reynolds numbers to observe the Kármán gait. Only within a certain range of flow velocities and cylinder sizes do vortices shed periodically and discretely enough to provoke a regular kinematic response. During low flow, fish avoid swimming behind cylinders, and at high flow (6 $L\,s^{-1}$), turbulence displaces fish from the wake, as revealed by sudden, high amplitude lateral excursions of the whole body. Although we confirmed the periodicity of the shed vortices with DPIV, at the Reynolds numbers of our experiment the three-dimensional cylinder wake is still subject to turbulence, axial flow and braid vortices (Blevins, 1990). We attribute interruptions during the otherwise steady Kármán gait to corrective, stabilizing movements used to compensate for these flow irregularities. Preliminary results from a cleaner, more stable wake generated by an automated, heaving cylinder verify that trout adopt a Kármán gait for longer periods with fewer corrective motions.

Kármán gait kinematics: evidence and implications of tuning

The hypothesis that fish are swimming behind cylinders only to take advantage of the reduced flow velocity (i.e. drafting) is not supported. On the contrary, the distinctive and consistent changes in axial body kinematics among different cylinder treatments supports the hypothesis that trout can tune their swimming kinematics to capture energy from vortices shed from cylinders. The body wave speed of trout behind small cylinders is lower than the body wave speed for similar sized trout swimming at the equivalent free stream speed (Webb et al., 1984), indicating that trout are not producing thrust in the same manner as when they swim in the free stream. The dramatic differences in the Kármán gait as compared to trout swimming in the free stream at 4.5 $L\,s^{-1}$ probably reflect different mechanisms of locomotion. Since the flow velocity behind the large cylinder is much lower than the free stream velocity, it can be argued that a more legitimate comparison would be between the kinematics of the Kármán gait behind the large cylinder and the kinematics of trout swimming at an

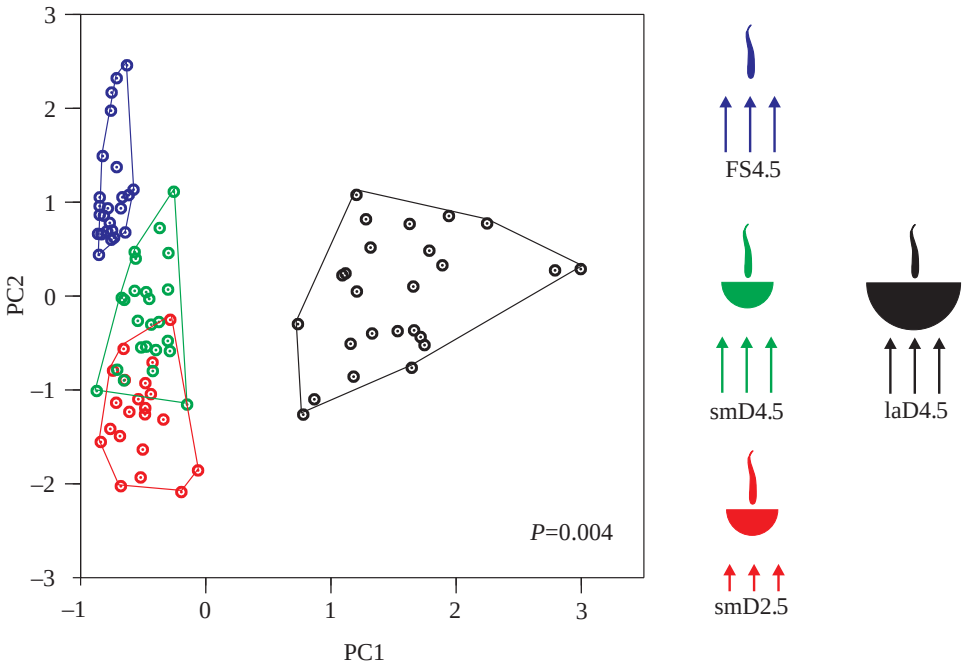

Fig. 9. Principal components analysis (PCA) on 13 kinematic variables for three downstream cylinder treatments and the free stream treatment. The variables that loaded high on PC1 were body amplitudes and wave speed, while the variables that loaded high on PC2 were tail-beat frequency, body wave velocity, and location of minimum amplitude. Results from a MANOVA show a significant difference among treatment means (Wilks' lambda, P=0.004, N=108). SmD4.5 is not statistically different (P>0.05) from smD2.5 along PC1, or from laD4.5 along PC2.

unobstructed flow equivalent to the reduced flow behind the large cylinder. Though we did not measure the tail-beat frequency and body wavelength of trout swimming at a free stream velocity of 2.7 $L\,s^{-1}$, values taken from similarly sized trout at a similar flow velocity (approx. 4.5 Hz and 0.97 L, respectively; Webb et al., 1984) are significantly higher and shorter than trout exhibiting the Kármán gait behind the large cylinder.

As mentioned above, the ratio of fish length to cylinder diameter is probably a key factor in determining the ability of fish to use the Kármán gait. Certain cylinder diameters will prevent fish of a given length from conforming their bodies to the size and spacing of vortices in the Kármán street. Contrary to one of our predictions, fish do not alter their body wavelength to match the wake wavelength prescribed by the cylinder. Why do trout consistently adopt a longer body wavelength than the wavelength dictated by the spacing of the vortices, and why does this relationship change with cylinder size? One explanation is that during the Kármán gait, trout position their head differently relative to a vortex than their tail. For example, by positioning the head to intercept a vortex and the tail to slalom around it, a trout will have a longer body wavelength than the cylinder wavelength despite interacting with each vortex in a consistent manner. Therefore, even though the wavelength along the body does not exactly match the wake wavelength for each of the three respective downstream cylinder treatments, the body wavelengths for trout subjected to the small cylinder treatments are still more similar to each other than either is to the wake wavelength behind the large cylinder. Since it is likely that trout utilize vortices by maintaining the body at an angle of attack relative to the localized region of vortical flow, then as vortex diameter increases, body wavelength may increase to insure this condition. In contrast to the wake wavelength, the shedding frequency, or the speed at which trout encounter vortices, has less of an effect on how trout shape their body into waves. What shedding frequency does dictate is the location of maximum body curvature, revealing that fish are not only conforming their bodies to interact with the shed vortices, but that they do so in a consistent way despite encountering differences in vortex size and strength.

Wake parameters differ in every respect between the small and large cylinder at high flow and yet trout show similar maximum body curvatures when swimming behind them. While body curvature may reflect the degree of body bending around large vortices shed from the large cylinder, the same magnitude of curvature for fish behind the small cylinder treatment may reflect a shift in station holding strategy to include active propulsion in addition to tuning. In support of this, maximum body curvature in trout swimming behind a small cylinder at high flow is no different from that of trout swimming with undulatory propulsion in the free stream at the same speed. For trout swimming behind small cylinders, more of the body moves laterally and by a greater factor relative to the center of mass than trout behind the large cylinder. The steeper amplitude envelope and larger relative midbody amplitude for trout behind the small cylinder treatments suggest that either body amplitude reflects a hydrodynamic relationship particular to shorter wake wavelengths, or that there is a degree of active undulation that is not present for trout swimming behind the large cylinder.

Head angles track vortex shedding frequency, further supporting the idea that body kinematics reflect interaction with vortices and not just undulatory propulsion through the reduced flow behind a cylinder (Fig. 7B). Fish subjected to treatments with the same shedding frequency adopt similar

head angles, suggesting that buffeting of the head by the vortices, combined with active contraction of anterior axial muscles, may be what determines the position of the head in the current. Alternatively, head angle may result from an entirely passive motion generated by the buffeting effect of the vortices.

Our calculations of slip (Lighthill, 1975) for trout behind cylinders are likely to be an overestimation because we considered swimming velocity equivalent to the nominal velocity (U_f), rather than the reduced velocity behind the cylinder. If slip is calculated by substituting the appropriate reduced velocity value behind a cylinder for fish swimming speed, then slip values for fish behind all cylinders are about half those of free stream swimming fish. Slip values may not be a useful metric of efficiency for fish swimming in perturbed environments since the proportion of the body wave that generates thrust propulsively is unknown. Thus, the faster body wave in trout behind cylinders may indicate vortex energy capture and wake buffeting rather than axial propulsion. If trout are holding station behind the large cylinder *via* some mechanism of vorticity control, they may be experiencing enhanced locomotory performance compared to trout swimming in the free stream (Anderson, 1996; Triantafyllou et al., 2000).

Hypothesized mechanism of the Kármán gait

Our results, which clarify the relationship between body kinematics and hydrodynamic parameters, lead us to propose that axial muscles may be largely inactive during the Kármán gait, especially behind the large cylinder. By what mechanism can a fish hold station or move upstream entirely passively if there is no net flow upstream? Drawing on a nautical analogy, we hypothesize that trout use their body like a sail to tack upstream. By changing the camber and angle of attack of the body to establish a differential pressure gradient (using the low pressure region of each oncoming vortex), it is possible to generate a net circulation around the body that, on average, keeps a component of the lift force directed upstream (Fig. 10). Thus, a major component of the Kármán gait may consist of a passive, lift-based mechanism that relies on the interaction of a body with the high velocity regions of shed vortices, similar to the mechanism of thrust production in foils oscillating in a vortex street (Streitlien and Triantafyllou, 1996).

Although not quantified in this study, it is possible that by positioning the body at a high angle of attack relative to the incident flow the lift force generated will direct the fish upstream as well as laterally, thereby causing the fish to hold position relative to

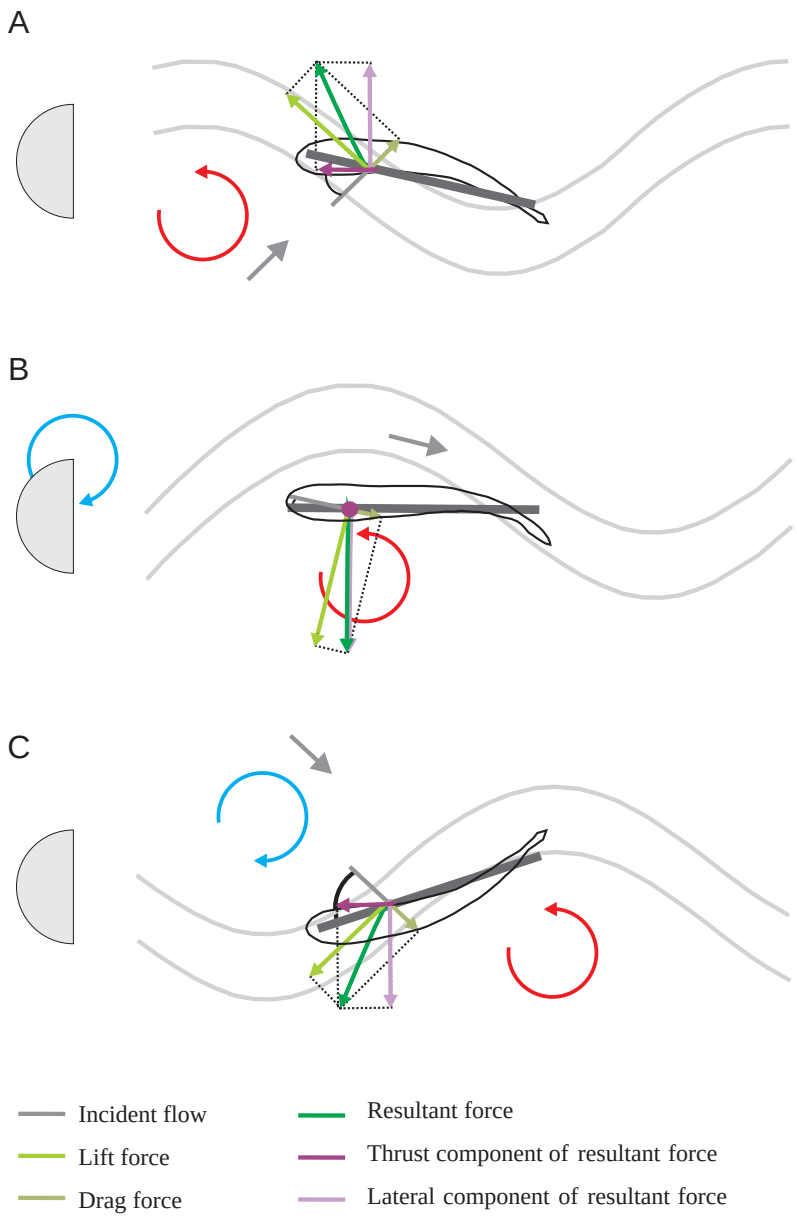

Fig. 10. Schematic of the hypothesized hydrodynamic mechanism of the Kármán gait. A low-pressure, counterclockwise vortex (red circle) is shed from the cylinder and approaches the head of the trout (A), causing the incident flow (gray arrow) to be directed at an angle to the body (simplified as the wide, dark gray line). The region of reduced flow behind the cylinder is illustrated by the sinusoidal light gray lines. The relatively large angle of attack of the body produces a lift force (light green arrow) normal to the path of the incident flow and a drag force (olive arrow) parallel to the flow. The resultant force (green arrow) can be decomposed into a forward component (purple arrow) and a lateral component (lavender arrow). At a small angle of attack (B), such as when a vortex is directly to the side of the body, the lift force causes the fish to only move laterally, since the thrust component of the lift force is zero (purple dot). A clockwise vortex (blue circle) is forming on the opposite side of the cylinder. The shed clockwise vortex is now just upstream of the trout in (C), and the counterclockwise vortex has drifted past the body of the trout. Force vectors are similar to that in A, only opposite in direction. Due to vorticity decay, the upstream vortex has a lower pressure than the downstream vortex, which may facilitate station holding.

the cylinder instead of drifting downstream (Fig. 10A). However, at times the incident flow may be parallel to the body (Fig. 10B). At this moment, the resultant lift vector can only be resolved into a lateral force, and the fish translates sideways but does not generate thrust. Over the course of one Kármán gait cycle, on average, the angle of attack of the body should generate enough thrust to overcome drag, allowing the fish to hold station while exhibiting large lateral oscillations of the body. Postural changes of the body such as these probably generate 'trimming' forces that stabilize the body in the presence of hydrodynamic perturbations (Webb, 2002).

An additional mechanism may contribute to the ability of trout to hold station using the Kármán gait. Since vorticity decays abruptly with distance from its source in turbulent systems (Glezer and Coles, 1990), the low-pressure region of a vortex returns to ambient as it drifts downstream. A trout positioning its head near an oncoming low-pressure vortex and its tail near a passing vortex (which has a relatively higher pressure) would be continuously drawn upstream relative to the flow, but hold station relative to the cylinder.

Bow wake

When trout swim in the low velocity, high-pressure region in front of a cylinder, their low tail-beat frequency, body wave speed and posterior body curvature suggest they are using the least amount of energy of all the treatments (Figs 5, 6). At the behavioral level, once fish discover the bow wake they do not leave, choosing to return immediately to the front rather than behind the cylinder if displaced. A similar phenomenon is seen in dolphins riding in the bow wake of ships (Scholander, 1959; Fejer, 1960; Bose and Lien, 1990). Slip values for bow wake fish indicate the highest mechanical efficiencies of all other treatments; however, since the flow velocity near the tail is not the same as along the anterior region of the body, calculating slip overestimates the forward swimming velocity of the fish. In addition, we do not know what portion of the tail-beat amplitude and frequency reflects propulsive thrust generation. Strouhal number is lowest for fish swimming in the bow wake, indicating a suboptimal swimming efficiency for what seems to be the most economical kinematic behavior of all the treatments. Since highly efficient swimmers have Strouhal numbers between 0.25–0.30 (Triantafyllou et al., 2000), the low value for bow wake fish (0.17) illustrates another unique mechanism of station-holding separate from the Kármán gait.

Conclusions and future directions

Our understanding of fish locomotion is dominated by detailed studies of steady swimming in homogenous, laboratory flow environments. The ubiquity of turbulence in nature provides ample justification for exploring the effects of hydrodynamic perturbations on fish swimming. Quantitatively assessing the reactions of fish to unpredictable hydrodynamic perturbations found in the natural environment is not currently within our grasp. Examining how fish alter their swimming behavior in response to periodic perturbations in the laboratory, however, is a productive intermediate step that promises to shed light on biomechanical questions regarding stability and control of aquatic animals, as well as stimulate practical applications for fisheries management. While the general tendency of salmonids to reduce locomotory costs by exploiting flow refugia has been shown in the field (Puckett and Dill, 1985; Heggenes, 1988; McMahon and Gordon, 1989; Fausch, 1993), the results of this paper detail the ability of trout to hold station by (1) adopting a novel gait to utilize the vortex street behind a cylinder and (2) swimming in the bow wake in front of a cylinder.

Ongoing investigations using electromyography, DPIV and oscillating hydrofoils should clarify the neuromuscular and hydrodynamic basis of the Kármán gait, enabling us to better address the mechanisms by which fish can make use of hydrodynamic perturbations created by inanimate objects in moving flow or by schooling fish. Current projects and key future questions include the following.

(1) What is the pattern of myotomal muscle activation during the Kármán gait? Electromyograms of trout across different cylinder treatments may reveal the proportion of the Kármán gait that reflects wake-specific tuning and the proportion that reflects propulsive undulation in a turbulent environment. Furthermore, changes in axial muscle activity, and hence body stiffness, may be expected to occur as wake parameters are altered. Energetics studies may show that trout swimming in predictably perturbed environments benefit when conditions favor energy capture from vorticity.

(2) Precisely what are the spatial and temporal relationships of the fish to the vortices during the Kármán gait? Does the body pass through the vortex cores or does it slalom around each vortex? Simultaneous visualization of body kinematics and flow behind the cylinder using DPIV will allow us to test the hypothesis presented in Fig. 10.

(3) What are the roles of other fins, particularly the pectoral fins, in effecting corrective movements? We have observed the pectoral fins to be constantly active during the Kármán gait, and believe they play a key role in station holding and resisting passive upstream movement in the suction region directly behind a cylinder.

(4) How do fish alter their kinematics when swimming in other vortex wakes? For instance, will fish tune when not given the option to draft? By adjusting the heave and pitch of an automated, oscillating foil, it may be possible to align vortices into a linear (*versus* staggered) array to eliminate the velocity deficit. Trout that choose to swim in this vortex wake must be tuning and not drafting, since vorticity is present without a region of reduced flow. Will fish swim in the drag wake created between two artificially generated thrust wakes, as proposed for the hydrodynamic mechanism of fish schooling?

We would like to thank Monica Daley, Eliot Drucker, Paul Webb, Ellen Freund, Franz Hover, Jen Nauen and Eric Tytell for constructive comments on the manuscript, and Laura Farrell for assistance in maintaining fish. We would also like to acknowledge Eric Tytell for use of his digitizing program. Support was provided by grants-in-aid of research from the

Society of Integrative and Comparative Biology to J.C.L. and NSF grant (IBN-9807012) to G.V.L.

References

Alexander, R. M. (1989). Optimization and gaits in the locomotion of vertebrates. *Physiol. Rev.* **69**, 1199-1227.

Anderson, J. M. (1996). Vorticity control for efficient propulsion. PhD thesis, Joint Program MIT/Woods Hole Oceanographic Institution.

Blake, R. W. (1983). *Fish Locomotion*. Cambridge: Cambridge University Press.

Blevins, R. D. (1990). *Flow Induced Vibration*, 2nd edition. Malabar, Florida: Krieger Publishing Company.

Bose, N. and Lien, J. (1990). Energy absorption from ocean waves: a free ride for cetaceans. *Proc. R. Soc. Lond. B* **240**, 591-605.

Drucker, E. G. and Lauder, G. V. (1999). Locomotor forces on a swimming fish: three-dimensional vortex wake dynamics quantified using digital particle image velocimetry. *J. Exp. Biol.* **202**, 2393-2412.

Fausch, K. D. (1993). Experimental analysis of microhabitat selection by juvenile steelhead (*Oncorhynchus mykiss*) and coho salmon (*Oncorhynchus kisutch*) in a British Columbia stream. *Can. J. Fish. Aquat. Sci.* **50**, 1198-1207.

Fejer, A. A. (1960). Porpoises and the bow-riding of ships under way. *Nature* **188**, 700-703.

Fish, F. E. (1999). Energetics of swimming and flying in formation. *Comments Theor. Biol.* **5**, 283-304.

Gerrard, J. H. (1966). Formation region of vortices behind bluff bodies. *J. Fluid Mech.* **25**, 401-413.

Gerstner, C. L. (1998). Use of substratum ripples for flow refuging by Atlantic cod, *Gadus morhua*. *Environ. Biol. Fishes* **55**, 455-460.

Gerstner, C. L. and Webb, P. W. (1998). The station-holding performance of plaice, *Pleuronectes platessa*, on artifical substratum ripples. *Can. J. Zool.* **76**, 260-268.

Glezer, A. and Coles, D. (1990). An experimental study of a turbulent vortex ring. *J. Fluid Mech.* **211**, 243-283.

Heggenes, J. (1988). Effects of short-term flow fluctuations on displacement of, and habitat use by, brown trout in a small stream. *Trans. Am. Fish. Soc.* **117**, 336-344.

Heggenes, J. (2002). Flexible summer habitat selection by wild, allopatric brown trout in lotic environments. *Trans. Am. Fish. Soc.* **131**, 287-298.

Jayne, B. C. and Lauder, G. V. (1995). Speed effects on midline kinematics during steady undulatory swimming of largemouth bass, *Micropterus salmoides*. *J. Exp. Biol.* **198**, 585-602.

Liao, J. and Lauder, G. V. (2000). Function of the heterocercal tail in white sturgeon: flow visualization during steady swimmming and vertical maneuvering. *J. Exp. Biol.* **203**, 3585-3594.

Lighthill, J. (1975). *Mathematical Biofluiddynamics*. Philadelphia: Society for Industrial and Applied Mathematics.

McLaughlin, R. L. and Noakes, D. L. G. (1998). Going against the flow: an examination of the propulsive movements made by young brook trout in streams. *Can. J. Fish. Aquat. Sci.* **55**, 853-860.

McMahon, T. E. and Gordon, F. H. (1989). Influence of cover complexity and current velocity on winter habitat use by juvenile coho salmon (*Oncorhynchus kisutch*). *Can. J. Fish. Aquat. Sci.* **46**, 1551-1557.

Nauen, J. C. and Lauder, G. V. (2002). Hydrodynamics of caudal fin locomotion by chub mackerel, *Scomber japonicus* (Scombridae). *J. Exp. Biol.* **205**, 1709-1724.

Pavlov, D. S., Lupandin, A. I. and Skorobogatov, M. A. (2000). The effects of flow turbulence on the behavior and distribution of fish. *J. Ichthyol.* **40**, S232-S261.

Puckett, K. J. and Dill, L. M. (1985). The energetics of feeding territoriality in juvenile coho salmon (*Oncorhynchus kisutch*). *Behaviour* **92**, 97-110.

Rayner, J. M. V. (1995). Dynamics of the vortex wakes of flying and swimming vertebrates. In *Biological Fluid Dynamics* (ed. C. P. Ellington and T. J. Pedley), pp. 131-155. Cambridge: Company of Biologists Limited.

Rice, W. R. (1989). Analyzing tables of statistical tests. *Evolution* **43**, 223-225.

Scholander, P. F. (1959). Wave-riding dolphins, how do they do it? *Science* **129**, 1085-1087.

Shuler, S. W., Nehring, R. B. and Fausch, K. D. (1994). Diel habitat selection by brown trout in the Rio Grande river, Colorado, after placement of boulder structures. *N. Am. J. Fish. Manage.* **14**, 99-111.

Streitlien, K. and Triantafyllou, G. S. (1996). Efficient foil propulsion through vortex control. *Amer. Inst. Aeronaut. Astronaut. J.* **34**, 2315-2319.

Sutterlin, A. M. and Waddy, S. (1975). Possible role of the posterior lateral line in obstacle entrainment by brook trout (*Salvelinus fontinalis*). *J. Fish. Res. Board Can.* **32**, 2441-2446.

Tobalske, B. W. (2000). Biomechanics and physiology of gait selection in flying birds. *Physiol. Biochem. Zool.* **73**, 736-750.

Triantafyllou, M. S., Triantafyllou, G. S. and Yue, D. K. P. (2000). Hydrodynamics of fishlike swimming. *Ann. Rev. Fluid Mech.* **32**, 33-53.

Vogel, S. (1994). *Life in Moving Fluids: The Physical Biology of Flow*, 2nd edition. Princeton: Princeton University Press.

Webb, P. W. (1991). Composition and mechanics of routine swimming of rainbow trout, *Oncorhynchus mykiss*. *Can. J. Fish. Aquat. Sci.* **48**, 583-590.

Webb, P. W. (1993). The effect of solid and porous channel walls on steady swimming of steelhead trout *Oncorhynchus mykiss*. *J. Exp. Biol.* **178**, 97-108.

Webb, P. W. (1998a). Entrainment by river chub *Nocomis micropogon* and smallmouth bass *Micropterus dolomieu* on cylinders. *J. Exp. Biol.* **201**, 2403-2412.

Webb, P. W. (1998b). Swimming. In *The Physiology of Fishes* (ed. D. H. Evans), pp. 3-21. Boca Raton, Florida: CRC Press.

Webb, P. W. (2002). Control of posture, depth, and swimming trajectories of fishes. *Integ. Comp. Biol.* **42**, 94-101.

Webb, P. W., Kostecki, P. T. and Stevens, E. D. (1984). The effect of size and swimming speed on the locomotor kinematics of rainbow trout. *J. Exp. Biol.* **109**, 77-95.

Weihs, D. (1973). Hydromechanics of fish schooling. *Nature* **241**, 290-291.

Wilga, C. D. and Lauder, G. V. (2000). Three-dimensional kinematics and wake structure of the pectoral fins during locomotion in leopard sharks *Triakis semifasciata*. *J. Exp. Biol.* **203**, 2261-2278.

Zar, J. H. (1999). *Biostatistical Analysis*, 4th edition. Englewood Cliffs: Prentice-Hall, Inc.

Zdravkovich, M. M. (1997). *Flow Around Circular Cylinders: A Comprehensive Guide Through Flow Phenomena, Experiments, Applications, Mathematical Models, and Computer Simulations*. Oxford: Oxford University Press.